Am J Transl Res 2023;15(7):4620-4628
www.ajtr.org /ISSN:1943-8141/AJTR0151779

Original Article

Clinical validation of an elastin-derived trifunctional peptide for skin regeneration

Jean-Daniel Abraham[1], Anais Vaissière[1], Christophe Desouches[2], Gaetan Thiery[3], Baptiste Bertrand[4], Bruno Alfandari[5], Ivan Courtois[6], Armand Azencot[7], Vincent Casoli[8], Pierre Haen[9], Thomas Colson[10], William Hornebeck[1], Didier Ritter[1]

[1]Regentis-Pharma, 8bis rue Gabriel Voisin, 51100 Reims, France; [2]Clinique Phenicia, 5 Boulevard Notre Dame, 13006 Marseille, France; [3]Centre Massilien de la face, 24 avenue du Prado, 13008 Marseille, France; [4]Hôpital de la Conception, 147 Bd Baille, 13005 Marseille, France; [5]Polyclinique Bordeaux Tondu, 143-153 rue du Tondu, 33082 Bordeaux, France; [6]Polyclinique Jean Villar, 56 av Maryse Bastié, 33520 Bruges, France; [7]Clinique chirurgicale Bel-Air, 138 Av de la république, 33073 Bordeaux, France; [8]CHU de Bordeaux, Pole des spécialités chirurgicales, Service de chirurgie plastique brûlés main, 33000 Bordeaux, France; [9]Hôpital d'instruction des armées Laveran (HIA), 34 Boulevard Laveran, 13013 Marseille, France; [10]122bis cours Gambetta, 13100 Aix en Provence, France

Received June 15, 2023; Accepted June 29, 2023; Epub July 15, 2023; Published July 30, 2023

Abstract: Aging is associated with progressive skin fragility, characterized in part by extracellular matrix (ECM) fragmentation. This degradation produces matrikines which have an impact on ECM rremodeling. Our group previously designed and characterized a trifunctional peptide (TFP), constituted of i) an elastokine motif $(VGVAPG)_3$, able to increase the expression of matrix constituent through the stimulation of the elastin-binding protein receptor, ii) a tripeptide inhibiting matrix metalloproteinase-1 activity (GIL), and iii) a linker domain acting as a competitive substrate for urokinase (RVRL). TFP was shown to activate the production of matrix constituents while inhibiting Matrix MetalloProtease MMP-1 *in vitro* on fibroblasts and *ex vivo* on skin explants. Objective: In the present study, TFP properties were evaluated in a clinical assay. Methods: Twenty-two volunteers applied a TFP-based cream on one hemi-face and a placebo-based cream on the other hemi-face, twice a day during 28 days, before undergoing a surgical lifting. Cutometry and skin relief measurements were performed at days 0 and 28, and skin explants from lifting surgery were used for histological analyses. Results: Cutometry and skin relief measurements reveal TFP firming properties and wrinkle depth decrease in 28 days on TFP- as compared to placebo-treated hemi-faces. These results are confirmed by histological analyses showing an increase of the ratio between basal lamina and stratum corneum. Furthermore, immunostaining of collagen reveals a modification of the ratio between type I and III collagens. Conclusion: The combined analysis of phenotypic and histologic parameters demonstrates a reorganization of the ECM towards a regenerative profile upon TFP treatment.

Keywords: Elastokines, extracellular matrix, collagen, cutometry, wrinkle, firmness

Introduction

The extracellular matrix (ECM) is a three-dimensional network of different connected proteins conferring to the skin its firmness, elasticity, flexibility, and resistance. It has a main role in cellular adhesion, differentiation, and cell growth [1] and gives the skin its unique regenerative properties [2]. It is constituted by 2 major proteins, collagen and elastin, produced by the fibroblasts, and each of them contributes to skin properties. The most predominant collagens of the skin are types I and III [3] and are organized in a network of fibrils conferring to the skin its resistance and its integrity thus providing skin firmness [4]. In contrast to elastin, collagen has a longer biosynthesis with age and its decrease occurs approximately at the age of 60 years [5]. The elastin confers elasticity to the skin as well as its capacity of deformation and resistance to stretching [6]. This protein has a remarkably long half-life, approximately 74 years. However, it has a low turnover, and its production is not

continuous. The peak of elastin biosynthesis is around 20 years and then it decreases from 30 years of age [7].

The degradation products of elastin are the elastokines which have the ability to bind the Elastin Binding Protein (EBP) receptor through a consensus motif xGxxPG [8-10]. This binding is at the origin of several regulation phenomena: fibroblast proliferation [11], angiogenesis [12], expression of MMPs [13], chemotaxis [14-16], and keratinocyte migration and differentiation [17, 18]. The identification of the xGxxPG sequence within elastokine, as the motif responsible for elastin-derived peptide biological activity, was a major breakthrough [19], since it is responsible for stimulating the synthesis of collagen 1 and 3 and to act in many facets of wound healing [20, 21]. With the aim of obtaining an elastokine with a strong regenerative power, while eliminating adverse effects, our group designed a TFP by coupling the sequence $(Val\text{-}Gly\text{-}Val\text{-}Ala\text{-}Pro\text{-}Gly)_3$ to the tripeptide GIL (Gly-Ile-Leu) designed to inhibit MMP-1. A peptide linker RVRL (Arg-Val-Arg-Leu) was introduced between these entities, which could recognize proteases of the plasminogen system. Our group previously demonstrated that TFP had the capacity to stimulate type I and type III collagens by dermal fibroblasts both in *in vitro* culture and *ex vivo* skin explants [22].

In the present study, the anti-aging performances of TFP were evaluated in a hemi-face 28-days clinical study on 22 volunteers that were monitored to study the wrinkle depth and the skin firmness evolution. These phenotypic observations were correlated *ex vivo* by immunohistochemistry on lifting explants on the same volunteers by detecting a differential collagen ratio between TFP- and placebo-treated hemi-faces. TFP impact on wrinkles and firmness could be related to an observed regenerative pattern highlighted by a modification of the ratio between types I and III collagens.

Materials and methods

Cream production

TFP ($(Val\text{-}Gly\text{-}Val\text{-}Ala\text{-}Pro\text{-}Gly)_3$-Arg-Val-Arg-Leu-Gly-Ile-Leu) was synthetized by Polypeptide (Strasbourg, France) under cosmetic grade production. Preliminary studies demonstrated an absence of mutagenicity (OECD 471 Ames test), phototoxicity (OECD 432), ocular intolerance (Het-Cam test), skin irritation (OECD 439) or skin sensitization (OECD 442E h-CLAT test) of TFP. TFP and placebo face creams were prepared by Cosinus (Dreux, France) and are composed of the same formulation of cosmetic solvents and emollients, with or without TFP (100 µg/ml) respectively.

In vivo study - clinical trial

This study was performed on human skin tissue obtained from surgical residues in full respect of the Declaration of Helsinki and Article L.1243-4 of the French Public Health Code. The clinical trial was registered under the number ANSM 2016-A00381-50 and was developed as a single-blind, multicenter, randomized and controlled trial conducted on 22 women (from 45 to 70 years old) who applied the two products, cosmetic creams with or without the TFP, either on the right or the left side of the face, twice a day for 28 days. After this period, they underwent a facelift surgery and the skin samples were recovered for histologic analyses.

Assessment of the biomechanical properties of the skin

Biomechanical properties of the skin, measured with a cutometer® MPA580 device, were carried out at day 0 and day 28 before and after application of the cosmetic products, on the volunteers' faces, at a pressure of 400 mbar, using a 2 mm diameter probe. Its operation mechanism bases on the suction and expansion of the skin by the measuring probe. The analysed parameters are a function of skin stretching and its return to its initial position. For the biomechanical properties measurements, the subjects are placed in a room with controlled environmental conditions in terms of relative humidity and temperature for at least 30 minutes before the instrumental measurements. The analysis of biomechanical properties of skin which have been examined consisted in determining the following parameters (**Figure 1**): immediate (Ue) and delayed (Uv) skin distension; gross elasticity of the skin (Uf), ie, the highest point of the curve; immediate

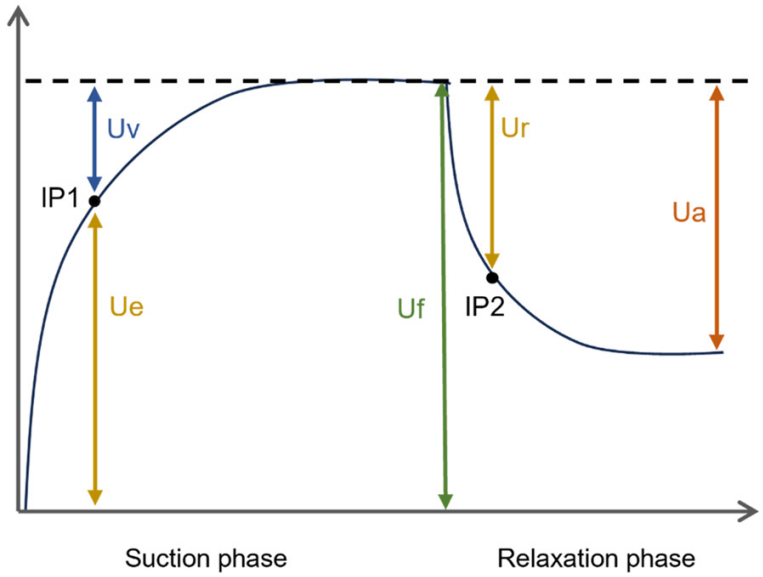

Figure 1. Biomechanical property measurement of the skin with a cutometer® MPA580 device. The resistance of the skin to the negative pressure (firmness) and its ability to return into its original position (elasticity) are displayed as curves (penetration depth in mm/time) in real time during the measurement. From these curves, different measurement parameters can be calculated: immediate (Ue) and delayed (Uv) skin distension; gross elasticity of the skin (Uf), ie, the highest point of the curve; immediate retraction (Ur), and length of skin retraction after elongation (Ua); IP, inflexion point.

retraction (Ur) and length of skin retraction after elongation (Ua) [23, 24].

Measurement of the depth of the wrinkles

Skin impressions were performed at D0 and D28 by mixing a silicone paste of SILFLO and a catalyst; the mixture thus obtained is applied to the skin surface, and left to dry for 10 minutes. This results in the negative silicone impression of the skin relief. The analysis is then carried out using an image analysis station equipped with Quantiride® software. The skin impression is illuminated by a grazing light (35°), generating shadows cast behind each wrinkle that are recorded using high-resolution digital camera. The QUANTIRIDES software analyses images obtained and determines the different characteristics of wrinkles (surface, length, depth).

Collection and treatment of skin removal after facelift

The surgical intervention is performed according to the classical technique of the surgeon. The surgical wastes, removed during the surgery, correspond to excess skin resulting from the laxity of the skin from the peri-auricular part. One piece of cutaneous excess of each side of the face was retrieved for further analyses. For histologic analyses, skin pieces from each side of the face (≥ 1 cm²) were immersed in a solution of 4% formalin at room temperature for 24 hours, then transferred in a solution of ethanol 70% and stored at room temperature before paraffin embedding and analysis. The paraffin sections of approximately 4 µm thick, were cut and placed on Superfrost Plus glass slides, and let dry overnight at 45°C (± 3°C) in an air oven before microscopy imaging.

Histological analyses

Hematoxylin-eosin (H&E) stained slides were digitized using the scanner Nanozoomer (HAMAMATSU) in bright field conditions, with the objective × 20. H&E stained slides were analysed to evaluate the morphometry of the basal lamina (separation between the epidermis and the dermis) by Halo® software (Indicalab). This analysis consisted in determining on the three parts of each sample, the length of the basal lamina and the length of the stratum corneum (normalization to take into account the variability of the sample size) to obtain the ratio: basal lamina/stratum corneum (BL/SC).

The labelling of collagens 1 and 3 on paraffin sections was simultaneously performed with the OPAL™4-color IHC (immunohistochemistry) kit from PerkinElmer® with rabbit polyclonal anti-collagen 1 and anti-collagen 3 antibodies (ORB319485 from Biorbyt and ab7778 from Abcam respectively). The immunostaining was optimized on Leica Bond RX platform. The antibody-labelled paraffin sections were then incubated with the fluorophore OPAL 690 (2018 Akoya Biosciences). The nuclei were labelled with DAPI. After a complete ICH and fluorescent labelling, the paraffin sections were scanned by the Vectra Polaris (PerkinElmer) with the objective × 20. The visualization, analysis, vali-

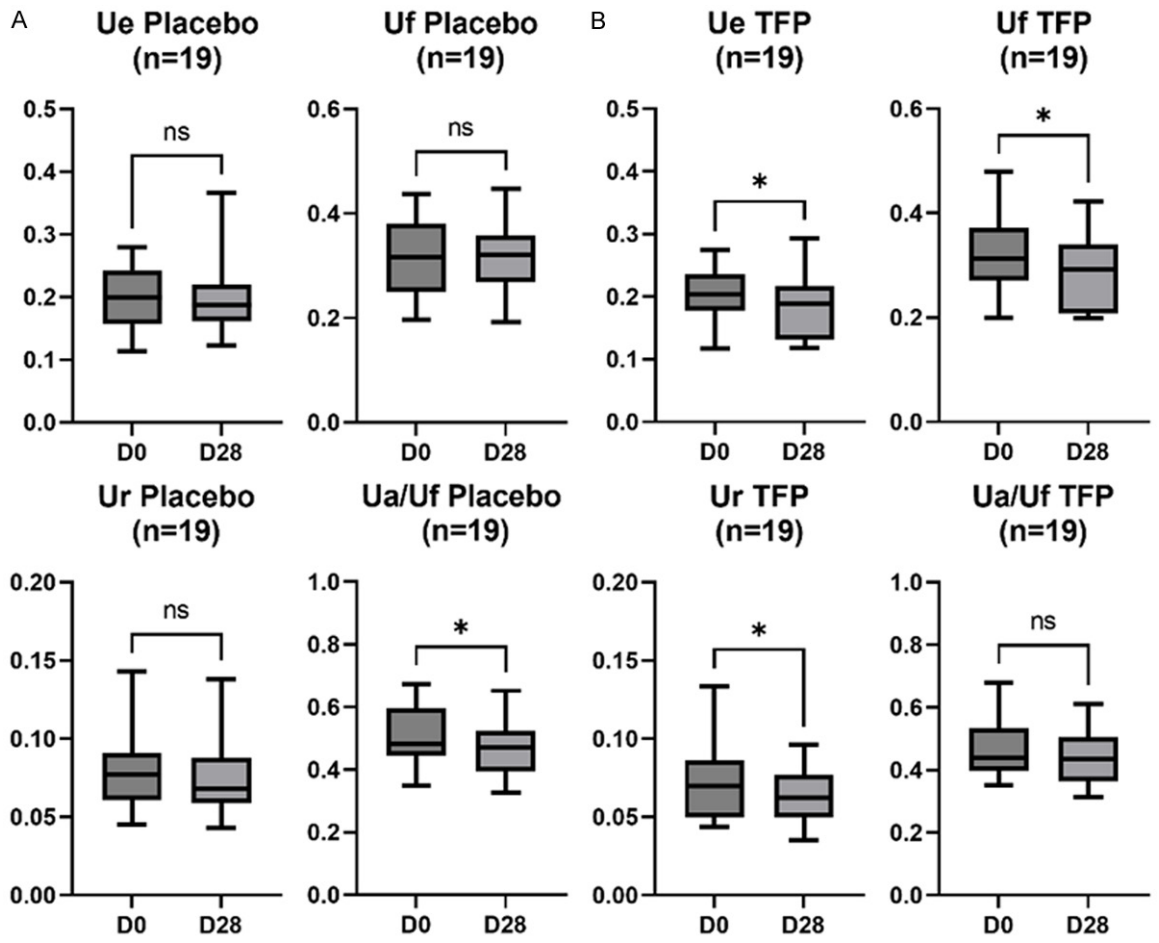

Figure 2. Assessment of the biomechanical properties of the skin. Biomechanical properties of the skin, measured by cutometry, were carried out at day 0 (D0) and day 28 (D28) before and after application of the cosmetic products. Evolution between D0 and D28 of Uf (final skin extension), Ue (immediate deformation), Ur (immediate retraction), and Ua/Uf (gross elasticity) are shown according to the treatment (Placebo, A, or TFP, B). *: *p*-value < 0.05; ns: not significant. TFP, trifunctional peptide.

dation, and quantification of images was performed with the software HALO® (Indicalabs).

Statistical analyses

All data are represented as the mean of 3 triplicates, and validated with %CV below 25%. The normality of the distribution of the data was verified by the Shapiro-Wilk test, at 5% risk. The data are analysed either by the paired t-Student test for a normal distribution or by the non-parametric Wilcoxon test for paired values in the opposite case.

Z combination was obtained by Linear Discriminant Analysis (LDA). LDA is a statistical method used for classification of problems where the goal is to find a decision boundary that separates different classes. LDA allows to determine a linear combination of features that maximally separates the classes [25].

In our study, $Z = 2 \times [LB/SC] + [Col3/Col1] - 2 \times [\text{wrinkle depth}] - 0.5 \times [(Uf_{D28}/Uf_{D0})] - 0.4 \times [Ue_{D28}/Ue_{D0})] - 0.1 \times [Ur_{D28}/Ur_{D0}]$.

Results

TFP improves skin firmness

Mechanical parameters of the skin were evaluated at D0 and D28 after TFP or placebo treatments. As shown in **Figure 2A**, no significant difference could be observed in placebo-treated hemi-faces in terms of skin immediate deformation (Ue), extensibility (Uf) or immedi-

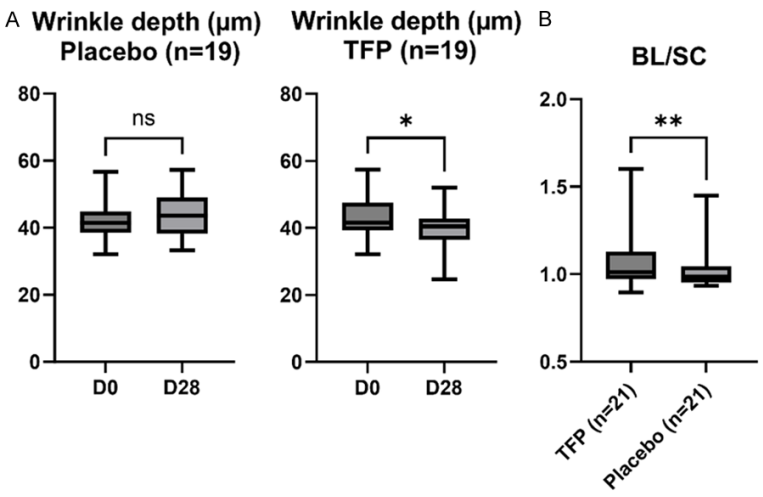

Figure 3. Skin wrinkle evolution after 28 days of treatment. A: Skin wrinkles were measured after skin silicone impression performed at D0 and D28 and analysis by Quantiride® software, on placebo-treated hemi-faces or TFP-treated hemi-faces; B: After surgical lifting, skin explants were analysed by histologic staining to evaluate the BL/SC ratio between skin basal lamina and stratum corneum in both conditions (TFP or placebo). **: *p*-value < 0.01; *: *p*-value < 0.05; ns: not significant. TFP, Trifunctional peptide; BL/SC, basal lamina/stratum corneum.

ate retraction (Ur). On the contrary, those 3 parameters significantly decreased in 28 days upon TFP treatment, showing an improvement of skin firmness ($P < 0.05$; **Figure 2B**). Conversely to other parameters, Ua/Uf ratio significantly decreased between D0 and D28 on placebo-treated hemi faces ($P < 0.05$; **Figure 2A**), not on TFP-treated hemi-faces (**Figure 2B**), which showed a lower decrease of skin viscoelasticity on TFP-treated hemi-faces.

Wrinkle depth decrease in TFP-treated hemi-faces

Wrinkle depth were measured using an image analysis station equipped with Quantiride® software. As shown in **Figure 3A**, no significant difference could be observed on placebo-treated hemi-faces between D0 and D28 (left panel), conversely to TFP-treated hemi-faces (*p*-value = 0.05, right panel). This result was confirmed by histologic evaluation on skin extracts after surgical lifting, on which basal lamina and stratum corneum were measured. As shown in **Figure 3B**, the BL/SC ratio is higher in TFP-treated hemi-faces as compared to placebo, due to a lower SC length as compared to BL length, confirming by histology that there is a wrinkle depth decrease ($P < 0.01$).

TFP modulates Col3/Col1 ratio

After skin explants embedding and slice preparation, a duplex immunohistological assay was performed in triplicate, to unambiguously detect collagen 1 and 3 and measure their relative quantity (**Figure 4A**). As shown on **Figure 4B**, the treatment of hemi-faces with the TFP preparation led to a significant increase of Col3/Col1 ratio as compared to placebo ($P = 0.001$).

TFP efficiency reaches 80%

Statistical combinatory analysis was conducted in order to evaluate the global efficiency of TFP in this study. As shown in **Figure 5A**, 80% of volunteers are positively impacted either in wrinkle depth, in skin firmness or collagen ratio by using TFP as compared to placebo. The virtual Z biomarker allows then a very high discrimination between both groups of samples (**Figure 5B**). Noteably, this discriminative value is not impacted by age of volunteers, as Z value is very significantly improved in TFP- vs placebo-treated samples, whether in volunteers below or above 62.5 y of age (**Figure 6**).

Discussion

The present study aimed at evaluating *in vivo* the anti-aging properties of an elastin-based trifunctional peptide (TFP) previously characterized *in vitro* on fibroblasts and *ex vivo* on skin explants. The great originality of this study lies in the fact that each patient's face is treated half with placebo and half with TFP. Thus, each patient was her own control, which allowed us to perform paired statistical analyses (Wilcoxon t-test), what greatly strengthens the results and conclusions.

Using a cutometer® MPA580 device, we were able to demonstrate an improvement of skin firmness (Uf and Ue decrease) and viscoelasticity (Ua/Uf ratio increase) by using TFP treatment after 28 days of application, as compared

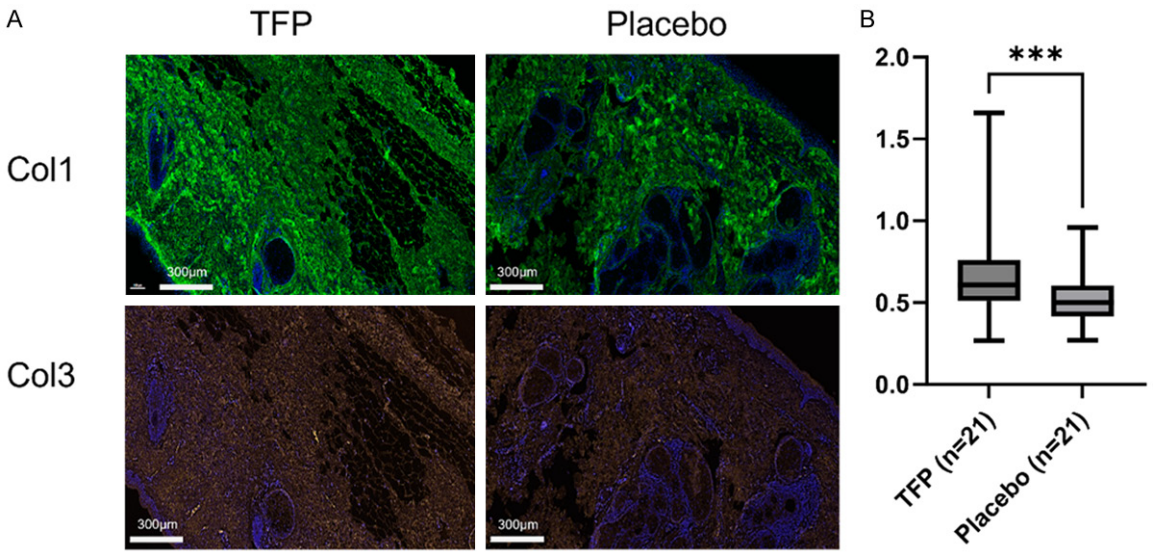

Figure 4. Col3/Col1 ratio increases upon TFP treatment. Immunohistological co-staining of type I and type III collagens on skin explants were performed simultaneously with a duplex protocol, allowing the rigorous evaluation of Col3/Col1 ratio on each slice; A: example of a coimmunostaining result (× 30); B: TFP treatment induces an increase in Col3/Col1 as compared to placebo. ***: *p*-value < 0.001; TFP, Trifunctional peptide.

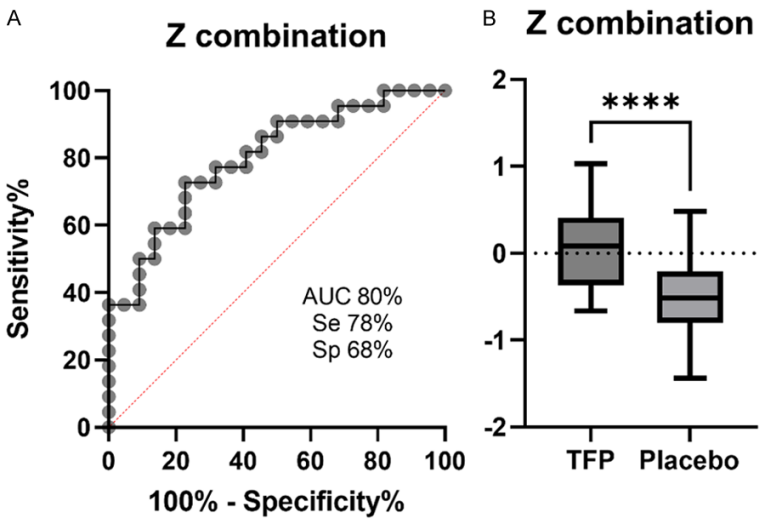

Figure 5. Z combination of skin physical parameters and IHC values allows a high discrimination between TFP and placebo. Physical and histologic parameters were combined in order to obtain a Z biomarker which allows a high discrimination between TFP and placebo conditions; A: ROC curve analysis of Z parameter allows an AUC of 80% (Se 78%; Sp 68%); B: Box-plot of Z combination between TFP and placebo groups; ****: *p*-value < 0.0001. TFP, Trifunctional peptide.

to placebo treatment. Thus, TFP demonstrates its anti-aging properties, as age-related changes consist of an overall decrease in firmness and elasticity [26-28], with a particular negative correlation between age and Ua/Uf ratio [29]. These results were confirmed by the measurement of the significant decrease of wrinkle depth by two complementary techniques: macroscopic analysis by Quantiride® software and microscopic histologic labelling of the basal lamina (BL) and stratum corneum (SC) after lifting surgery.

Using immunohistochemical analyses, we were able to establish that these phenotypic changes in the skin could be due to a reorganization of collagen fibers within the extracellular matrix. Indeed, the relative ratio of type III collagens as compared to type I (Col3/Col1 ratio) was increased in TFP-treated hemi-faces. This modification is of importance, as it confirms *in vivo* our previous results observed *in vitro* [22]. This result demonstrates the regenerative properties of TFP. Indeed, type I collagen is the predominant collagen in normal human skin and exceeds type III collagen by a ratio of 4:1, whereas this ratio decreases to 2:1 in wound healing, due to an early increase in the deposi-

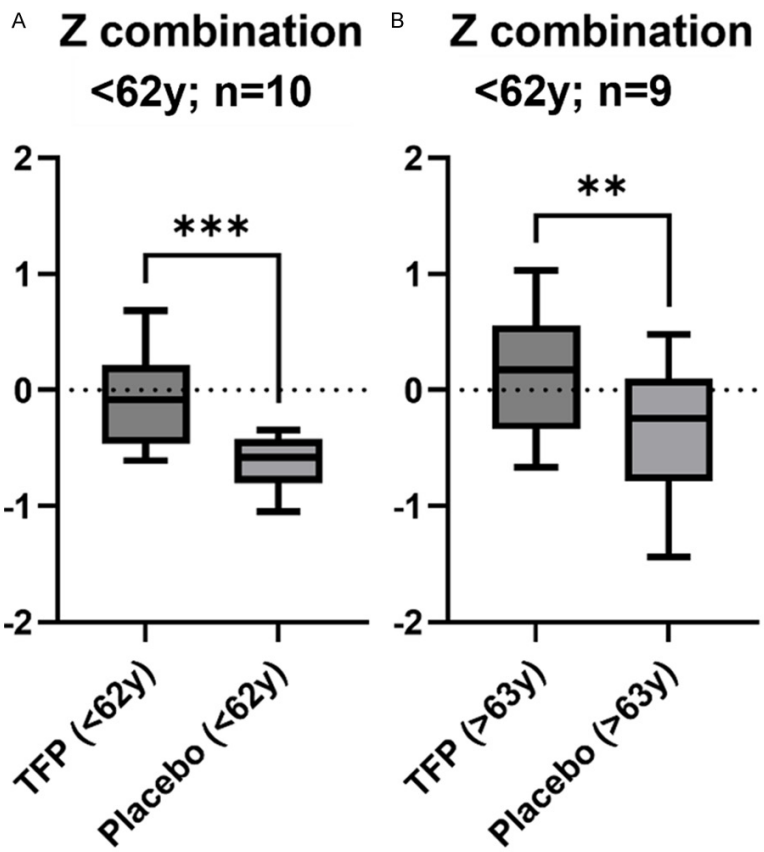

Figure 6. Z combination allows a high discrimination between TFP and placebo, whatever the age of the volunteers. Physical and histologic parameters were combined in order to obtain a Z biomarker that allows a high discrimination between TFP and placebo conditions; A: Volunteers below 62 y of age; B: Volunteers above 63 y of age; ***: *p*-value < 0.001; **: *p*-value < 0.01. TFP, Trifunctional peptide.

tion of type III collagen. Thus, early deposition of type III collagen in wounds appears as a crucial step for the evolution of the healing process. Conversely, diminished type III collagen promotes myofibroblast differentiation and increases scar deposition in cutaneous wound healing [30]. Likewise, it was shown that hypertrophic and immature scars could result in a lower level of collagen type III and a higher ratio of Col1/Col3 [31, 32]. This overall literature demonstrates that an increase in Col3/Col1 ratio is associated with a positive phenotype in matrix regeneration.

By using Linear Discriminant Analysis (LDA), we were able to determine a linear combination of features (Z combination) that maximally separates TFP- vs placebo-treated samples [25]. The discriminative power of this virtual biomarker allows us to claim a high efficiency of TFP, as at least 80% of the tested volunteers displayed a positive response to the treatment. Furthermore, as shown in **Figure 6**, Z combination allows a very significant discrimination between TFP- and placebo-treated hemi-faces, whatever the age of the volunteers, above or below 62.5 y. This analysis is of importance, as it demonstrates the properties of TFP to improve skin regeneration at any age.

In conclusion, our study demonstrates unambiguously the regenerative properties of TFP, demonstrating an anti-age macroscopic impact and molecular extracellular matrix reorganization.

Disclosure of conflict of interest

JDA and AV are Regentis Pharma employees. WH and DR are consulting experts for Regentis Pharma. Other authors have no conflict of interest to declare.

Address correspondence to: Jean-Daniel Abraham, Regentis-Pharma, 8bis rue Gabriel Voisin, 51100 Reims, France. E-mail: jean-daniel.abraham@regentis-pharma.com

References

[1] Theocharis AD, Skandalis SS, Gialeli C and Karamanos NK. Extracellular matrix structure. Adv Drug Deliv Rev 2016; 97: 4-27.
[2] Birch HL. Extracellular matrix and ageing. Subcell Biochem 2018; 90: 169-190.
[3] Gelse K, Pöschl E and Aigner T. Collagens-structure, function, and biosynthesis. Adv Drug Deliv Rev 2003; 55: 1531-1546.
[4] Yang W, Sherman VR, Gludovatz B, Schaible E, Stewart P, Ritchie RO and Meyers MA. On the tear resistance of skin. Nat Commun 2015; 6: 6649.
[5] Varani J, Dame MK, Rittie L, Fligiel SE, Kang S, Fisher GJ and Voorhees JJ. Decreased collagen production in chronologically aged skin: roles

of age-dependent alteration in fibroblast function and defective mechanical stimulation. Am J Pathol 2006; 168: 1861-1868.
[6] Pasquali-Ronchetti I and Baccarani-Contri M. Elastic fiber during development and aging. Microsc Res Tech 1997; 38: 428-435.
[7] Shapiro SD, Endicott SK, Province MA, Pierce JA and Campbell EJ. Marked longevity of human lung parenchymal elastic fibers deduced from prevalence of D-aspartate and nuclear weapons-related radiocarbon. J Clin Invest 1991; 87: 1828-1834.
[8] Blanchevoye C, Floquet N, Scandolera A, Baud S, Maurice P, Bocquet O, Blaise S, Ghoneim C, Cantarelli B, Delacoux F, Dauchez M, Efremov RG, Martiny L, Duca L and Debelle L. Interaction between the elastin peptide VGVAPG and human elastin binding protein. J Biol Chem 2013; 288: 1317-1328.
[9] Heinz A. Elastases and elastokines: elastin degradation and its significance in health and disease. Crit Rev Biochem Mol Biol 2020; 55: 252-273.
[10] Heinz A, Jung MC, Duca L, Sippl W, Taddese S, Ihling C, Rusciani A, Jahreis G, Weiss AS, Neubert RH and Schmelzer CE. Degradation of tropoelastin by matrix metalloproteinases--cleavage site specificities and release of matrikines. FEBS J 2010; 277: 1939-1956.
[11] Kamoun A, Landeau JM, Godeau G, Wallach J, Duchesnay A, Pellat B and Hornebeck W. Growth stimulation of human skin fibroblasts by elastin-derived peptides. Cell Adhes Commun 1995; 3: 273-281.
[12] Bellon G, Martiny L and Robinet A. Matrix metalloproteinases and matrikines in angiogenesis. Crit Rev Oncol Hematol 2004; 49: 203-220.
[13] Brassart B, Randoux A, Hornebeck W and Emonard H. Regulation of matrix metalloproteinase-2 (gelatinase A, MMP-2), membrane-type matrix metalloproteinase-1 (MT1-MMP) and tissue inhibitor of metalloproteinases-2 (TIMP-2) expression by elastin-derived peptides in human HT-1080 fibrosarcoma cell line. Clin Exp Metastasis 1998; 16: 489-500.
[14] Sarfati I, Lopes D, Murphy EA, Rao S and Cohen JR. Inhibition by protease inhibitors of chemotaxis induced by elastin-derived peptides. J Surg Res 1996; 61: 84-88.
[15] Senior RM, Griffin GL, Mecham RP, Wrenn DS, Prasad KU and Urry DW. Val-Gly-Val-Ala-Pro-Gly, a repeating peptide in elastin, is chemotactic for fibroblasts and monocytes. J Cell Biol 1984; 99: 870-874.
[16] Senior RM, Griffin GL and Mecham RP. Chemotactic activity of elastin-derived peptides. J Clin Invest 1980; 66: 859-862.
[17] Donet M, Brassart-Pasco S, Salesse S, Maquart FX and Brassart B. Elastin peptides regulate HT-1080 fibrosarcoma cell migration and invasion through an Hsp90-dependent mechanism. Br J Cancer 2014; 111: 139-148.
[18] Fujimoto N, Tajima S and Ishibashi A. Elastin peptides induce migration and terminal differentiation of cultured keratinocytes via 67 kDa elastin receptor in vitro: 67 kDa elastin receptor is expressed in the keratinocytes eliminating elastic materials in elastosis perforans serpiginosa. J Invest Dermatol 2000; 115: 633-639.
[19] Brassart B, Fuchs P, Huet E, Alix AJ, Wallach J, Tamburro AM, Delacoux F, Haye B, Emonard H, Hornebeck W and Debelle L. Conformational dependence of collagenase (matrix metalloproteinase-1) up-regulation by elastin peptides in cultured fibroblasts. J Biol Chem 2001; 276: 5222-5227.
[20] Antonicelli F, Bellon G, Lorimier S and Hornebeck W. Role of the elastin receptor complex (S-Gal/Cath-A/Neu-1) in skin repair and regeneration. Wound Repair Regen 2009; 17: 631-638.
[21] Antonicelli F, Bellon G, Debelle L and Hornebeck W. Elastin-elastases and inflamm-aging. Curr Top Dev Biol 2007; 79: 99-155.
[22] Attia-Vigneau J, Terryn C, Lorimier S, Sandre J, Antonicelli F and Hornebeck W. Regeneration of human dermis by a multi-headed peptide. J Invest Dermatol 2014; 134: 58-67.
[23] Dobrev HP. A study of human skin mechanical properties by means of cutometer. Folia Med (Plovdiv) 2002; 44: 5-10.
[24] Léger D, Gauriau C, Etzi C, Ralambondrainy S, Heusèle C, Schnebert S, Dubois A, Gomez-Merino D and Dumas M. "You look sleepy..." the impact of sleep restriction on skin parameters and facial appearance of 24 women. Sleep Med 2022; 89: 97-103.
[25] McLachlan GJ. Discriminant analysis and statistical pattern recognition: mclachlan/discriminant analysis & pattern Recog. Hoboken, NJ, USA: John Wiley & Sons, Inc.; 1992.
[26] Krueger N, Luebberding S, Oltmer M, Streker M and Kerscher M. Age-related changes in skin mechanical properties: a quantitative evaluation of 120 female subjects. Skin Res Technol 2011; 17: 141-148.
[27] Langton AK, Graham HK, Griffiths CEM and Watson REB. Ageing significantly impacts the biomechanical function and structural composition of skin. Exp Dermatol 2019; 28: 981-984.
[28] Piérard GE, Kort R, Letawe C, Olemans C and Piérard-Franchimont C. Biomechanical assessment of photodamage: Derivation of a cutaneous extrinsic ageing score. Skin Res Technol 1995; 1: 17-20.
[29] Ohshima H, Kinoshita S, Oyobikawa M, Futagawa M, Takiwaki H, Ishiko A and Kanto H. Use of

Cutometer area parameters in evaluating age-related changes in the skin elasticity of the cheek. Skin Res Technol 2013; 19: e238-242.
[30] Volk SW, Wang Y, Mauldin EA, Liechty KW and Adams SL. Diminished type III collagen promotes myofibroblast differentiation and increases scar deposition in cutaneous wound healing. Cells Tissues Organs 2011; 194: 25-37.
[31] Perez-Aso M, Mediero A and Cronstein BN. Adenosine A2A receptor (A2AR) is a fine-tune regulator of the collagen1:collagen3 balance. Purinergic Signal 2013; 9: 573-583.
[32] Zhou Y, Zhao Y, Du H, Suo Y, Chen H, Li H, Liang X, Li Q and Huang X. Downregulation of CFTR Is Involved in the Formation of Hypertrophic Scars. Biomed Res Int 2020; 2020: 9526289.